Egyptian Journal of Chemistry

http://ejchem.journals.ekb.eg/

Adsorptive Desulfurization of Model Oil by Ag Nanoparticles-Modified Eichhornia Crassipes: Equilibrium, Kinetics, and Thermodynamic Studies

Ali J. Salim [a]*, Yousif K. Al-Haidarie [b], Mohammad I. Nasir [c]*

[a] *Department of Chemistry, College of Science, Mustansiriyah University, Baghdad-Iraq*
[b] *Al-Turath University College, Baghdad-Iraq*
[c] *Analysis Management Section, Petroleum R &D Center, Baghdad, Iraq*

Abstract

Sulfur derivatives are major contaminants in hydrocarbon fuels. Sulfur emissions from fuel are a major environmental concern, and many countries are enacting legislation to limit them. The presence of sulfur species in fuels are clearly a major issue in air pollution, airborne particulate emissions, pose industrial challenges (i.e. corrosion of equipment and deactivation of catalysts) and endangering health public. In this study low-cost agricultural (Eichhornia crassipes) adsorbent impregnated with silver was used to remove the major refractory sulfur compounds, such as thiophene (T), benzothiophene (BT) and dibenzothiophene (DBT) from n-heptane as the model fuel. Chemical and physical properties of the as-synthesized adsorbent were investigated by (Scanning Electron Microscopy) SEM, (X-Ray Diffraction) XRD, (Brunauer–Emmett–Teller) BET method, and (Fourier Transform Infrared spectroscopy) FTIR. The parameters such as initial concentration of sulfur compounds, contact time, and Ag Nano Composite dosage affecting the removal of sulfur compounds from model oil have been investigated. The adsorption capacities of the Ag Nano composites are 5.58 mg-S/g, 5.89 mg-S/g, and 6.83 mg-S/g, respectively, At various temperatures, the Langmuir, Freundlich, Temkin, and Dubinin–Radushkevich isotherms were used to describe equilibrium adsorption at various temperatures, with the Langmuir isotherm agreeing with the experimental equilibrium results. Pseudo-first-order, pseudo-second-order, intraparticle diffusion, and Elovich kinetic models are all investigated. The pseudo-second order model was found to be the best fit for the adsorption equilibrium and defining the kinetics. Finally, at various temperatures, the thermodynamic functions of adsorption reactions were estimated. The results showed that the adsorption process was spontaneous because the free energy (ΔG) was negative, and the reaction was exothermic and had kinetic energy (randomness) since the free energy (ΔG) was positive.

Keywords: Adsorptive Desulfurization, Ag Nano Composite

1. Introduction

Sulfur compounds in the form of sulfides, thiols, alkylated benzothiophene (BT), and others are naturally present in raw petroleum products. The presence of sulfur is able to promote catalyst poisoning in engines, corroding parts for internal combustion and lowering the efficiency of combustion. [1]. The formation of sulfur oxides (SOx) from the ignition of fuel oil leads to various problems such as acid rain, smog, and pulmonary problems [2–4]. Many countries are implementing stringent environmental regulations to limit the total sulfur content in fuel products. The European Union and the United States Environmental Protection Agency have set maximum sulfur standards for diesel oil at 10 and 15 ppmw, respectively [5,6]. Industrially, the elimination of sulfur is carried out through a process called hydrodesulfurization (HDS). Co–Mo/Al2O3, Ni–Mo/Al2O3, and Ni–W/Al2O3 catalysts are used in HDS.

However, attaining such a regulation is technically challenging because the conventional hydrodesulfurization (HDS) technique cannot achieve

*Corresponding author e-mail: alijs82@uomustansiriyah.edu.iq.; (Ali Jabber Salim)
Receive Date: 30 January 2022, **Revise Date:** 01 May 2022, **Accept Date:** 15 May 2022, **First Publish Date:** 15 May 2022
DOI: 10.21608/EJCHEM.2022.119149.5361

the target regulation, and poorly isolates the aromatic refractory sulfur compounds from fuel. Furthermore, HDS is uneconomical due to the high temperatures, pressures, and catalyst dosage requirements [7, 8].Several techniques have been developed to address the limitations of HDS, the most notable of which are: bio desulfurization, oxidative desulfurization, membrane separation, ionic liquid desulfurization, and adsorptive desulfurization [9,10]. Adsorption desulfurization has several advantages over other techniques due to its facile and mild operating conditions. Moreover, its ability to isolate the refractory sulfur compounds efficiently using relatively cheap adsorbents has made the technique widely appreciated. The focus of researchers in the past decades has been the search for more porous adsorbents that will be reasonably cheap, highly selective, consistently reliable, productively efficient, and easily regenerable [11, 12].

Despite the organic pollutants, sorbent materials are characterized by most of these properties. However, they are non-biodegradable and environmentally unfriendly. So, they are substituted by natural sorbents such as rice straw, cotton, peat moss, cotton grass, kapok, and water hyacinth, which have been examined as eco-friendly sorbents for spilled oil. Besides, these agricultural-based materials are inexpensive. Some of these agricultural products are waste materials, so, their reuse will save on waste disposal fees [13].

Water hyacinths (Eichhornia crassipes) are classified as agricultural waste plants due to their rapid growth rate and huge quantities that have a negative impact on aquatic life. However, as a natural biosorbent material, this plant has a high absorption rate, and it has many other amazing properties such as low cost, availability, and reusability [14].Recently, production of highly porous activated carbon with a large surface area from agricultural wastes has been focused on more environmental concerns and protection [15–16].

Accordingly, the production of nanocomposite from water hyacinth has potential economic and environmental impacts. First, it converts unwanted, low-value aquatic plants into useful, high-value sorbents. Second, the production of Nano-composites represents an adsorbent material for desulfurization. The work involves selecting optimum conditions for maximum removal of thiophene, benzothiophene (BT), and dibenzothiophene (DBT) in a model fuel, such as contact time, initial sulfur concentration, and adsorbent dosage, for the adsorption of desulfurization of thiophene, benzothiophene (BT), and dibenzothiophene (DBT) in a model fuel. The value of kinetic and thermodynamic research in figuring out the reaction mechanism and thermodynamic parameters was thought about.

2.1 Instrumentation

Scanning Electron Microscope(SEM) model Philips XL series 30, Shimadzu-XRD 6000, UV–visible spectrometer, BET surface area measurements BELSORP-mini II, (Spain), CARY 100 Conc, Shimadzu 8400 FTIR, Water bath shaker type Lab. Companion BS-11, digital scale KERN-ABS were employed in this work.

2.2- MATERIALS AND METHODS

Dibenzothiophene (DBT, 98%), Benzothiophene (BT, 98%), Thiophene (T, 99%), Hydrochloric acid (37%),n-heptane (99%) Sigma Aldrich, Silver nitrate (99%), Sigma Aldrich and Sodium hydroxide (98%) Fulka were of analytical grade and used as received.

2.3-Preparation of Biosorption

Plants of the fresh water hyacinth (Eichhornia crassipes) (EC) were taken from Baghdad's Dijla River. rinsed completely with distilled water and dried for four days in the sun. The powder was then processed and sieved to a particle size of 150 microns. Water hyacinth powder was shaken with distilled water for an overnight period before being filtered and dried in an air oven at 80 °C. It was then carbonized at 500 °C for 2 hours with 10 grams of Eichhornio crassipes in a crucible, and sieved to a particle size of 75 microns.

2.4- Loading of Ag nanoparticles on Eichhornia crassipes.

The desulfurization adsorbent was made using the co-precipitation technique. In a typical process, a 0.2 M solution of Ag $(NO_3)_2$ was combined with 10 g of Eichhornia crassipes and 10 g of urea in stoichiometric quantities. Adjust the pH of the mixture by adding 1M of NaOH solution (drop by drop) until it reaches 8. The adsorbent was agitated for 5 hours at 25 C^o using mechanical stirrers (3000 rpm), then filtered, washed, and dried in an oven at 90 degrees Celsius for 24 hours. The dry solid mass was crushed into a fine powder and screened using a sieve with a mesh size of 150 microns. The adsorbent was calcined for 4–5 hours at 500 C^o before being stored in a vacuum dissicator. [17].

2.5-Preparation of Model diesel oils

Model diesel oils were made by dissolving Thiophene, Benzothiophene, and Dibenzothiophene in n-heptane, with an initial S-content of 1000 ppm for each. All of these stock solutions were immediately employed in the adsorption studies that followed.

2.6- Analytical method

UV-Vis spectrophotometer was used to evaluate the concentrations of (Thiophene, BT, and DBT in n-heptane as a model fuel) before and after adsorption.

2.7-Adsorption and Kinetics Studies

The adsorption rates of thiophene, BT, and DBT in n-heptane as a model fuel using Ag Nano Composite were studied. It is necessary to examine the adsorbent dosage, initial concentration, and agitation time. Ag Nano Composite adsorption of (Thiophene, BT, and DBT in n-heptane) was studied at various contact times (30, 60, 90, 120, 150, 180, 210, and 240 min). During each agitation interval, the bottle's contents (thiophene, BT, and DBT) were filtered and the equilibrium concentration of each was determined. Using a mechanical shaker and several glass bottles covered with different amounts of adsorbent (0.05–0.5 g), we studied the influence of the adsorbent dose on the adsorption of (Thiophene, BT, and DBT) on the amount of Ag Nano Composite. Adsorption capacity (qe) was calculated through the mass balance expression equation. (1) Equation [18].

$$q_e = \frac{(C_i - C_e) \times V}{M} \quad \ldots\ldots\ldots\ldots\ldots\ldots\ldots\ldots(1)$$

$$R\% = \frac{(C_i - C_e)}{C_i} \times 100 \quad \ldots\ldots\ldots(2)$$

Where C_o is the initial concentration, Ce is the concentration of sulfur compounds in solution (mg/L) at equilibrium, C_t is the concentration of sulfur compounds in solution (mg/L) at time t in solution, V is the volume of initial sulfur compounds solution used (L) and M is the mass of adsorbent used (g). Furthermore, the kinetics of adsorption was studied by analyzing the adsorptive uptake of thiophene, BT, and DBT at different time intervals. The pseudo–first–order, pseudo–second–order, and intrapartical diffusion model equations were fitted to the kinetics of adsorption (Thiophene, BT, and DBT) onto the Ag Nano Composite. The linearity of each model, when plotted, was used to find out how suitable each model was for illustrating the adsorption. A UV-Visible spectrophotometer was used to measure the adsorbed amounts of thiophene, BT, and DBT at maximum wavelengths of 226 nm, 297 nm, and 325 nm, respectively.[19] removal efficiency R% of thiophene, BT, and DBT were calculated using the following equations (2). Adsorption isotherm tests were performed by shaking the Ag Nano Composite (0.2 g) with 50 ml of (Thiophene, BT, and DBT) (10–80) mg/L solution for 180 minutes at various temperatures (25, 35, 45, 55 ^{o}C).

3. Results and discussion

3.1. Adsorbent characterization

The study found that before the calcination process, Eichhornio crassipes had removal efficiencies of 13, 10, and 7% for DBT, thiophene, and BT, respectively. But after the calcination process, the removal efficiencies for DBT, thiophene, and BT are 27, 18, and 12%, respectively. When the Ag Nano Composite is utilized, the removal efficiencies for DBT, thiophene, and BT are 87, 81, and 72.5%, respectively. We noticed a big difference in the removal percentage when using the Ag Nano Composite, so the Ag nanocomposite was focused on in the adsorption process of organic sulfur compounds.

3.1.1-FESEM and EDX Analysis of Adsorbents

EC and Ag Nano Composite were studied by scanning electron microscopy (FESEM) as it gives information about surface morphology. FESEM images show before calcination raw EC (Fig. 1a), after calcination raw EC (Fig. 1b), Ag Nano Composite (Fig. 1c) and Ag Nanoparticle (Fig. 1d). FESEM images show before calcination raw EC exhibited a smooth and homogeneous morphology. After calcination raw EC has a homogeneous spherical shape, more porous morphology, and non-uniform textural properties, whereas the Ag Nano Composite adsorbent revealed a soft and less porous morphology. The surface morphology of EC materials is different from that of Ag Nano Composite and may significantly alter the physicochemical properties and porosity of the materials. EC has clear pores, and when loading silver nanoparticles, a change in surface shape is evident, as silver nanoparticles cover all the pores on the surface of EC. The FESEM images of the AgNP are shown in Fig. (1e-h). the surface morphology of silver nanoparticles is relatively spherical and regular. In the present study, the diameter of the particle size ranges from 27.58 nm to 38.72 nm. Similar results were also reported for synthesized silver nanoparticles [20]. For this purpose, EDX was performed on before calcination raw EC, after calcination raw EC, and Ag Nano Composite to determine their elemental composition. Each of the elements in EC, Ag Nano Composite, and Ag Nanoparticle are shown in the

figure. In addition to silicon, oxygen, and aluminum, the EDX spectrum of EC shows sodium, calcium, potassium, calcium, and carbon in the sample as well. Accumulations of silver, oxygen, and very little calcium are found in the Ag Nano Composite EDX spectrum data. Ag nanoparticles account for the most silver in the EDX spectrum of the Ag Nano Composite. The EDX spectrum of the Ag Nano Composite shows that silver nanoparticles were able to be added to the EC, which is good.

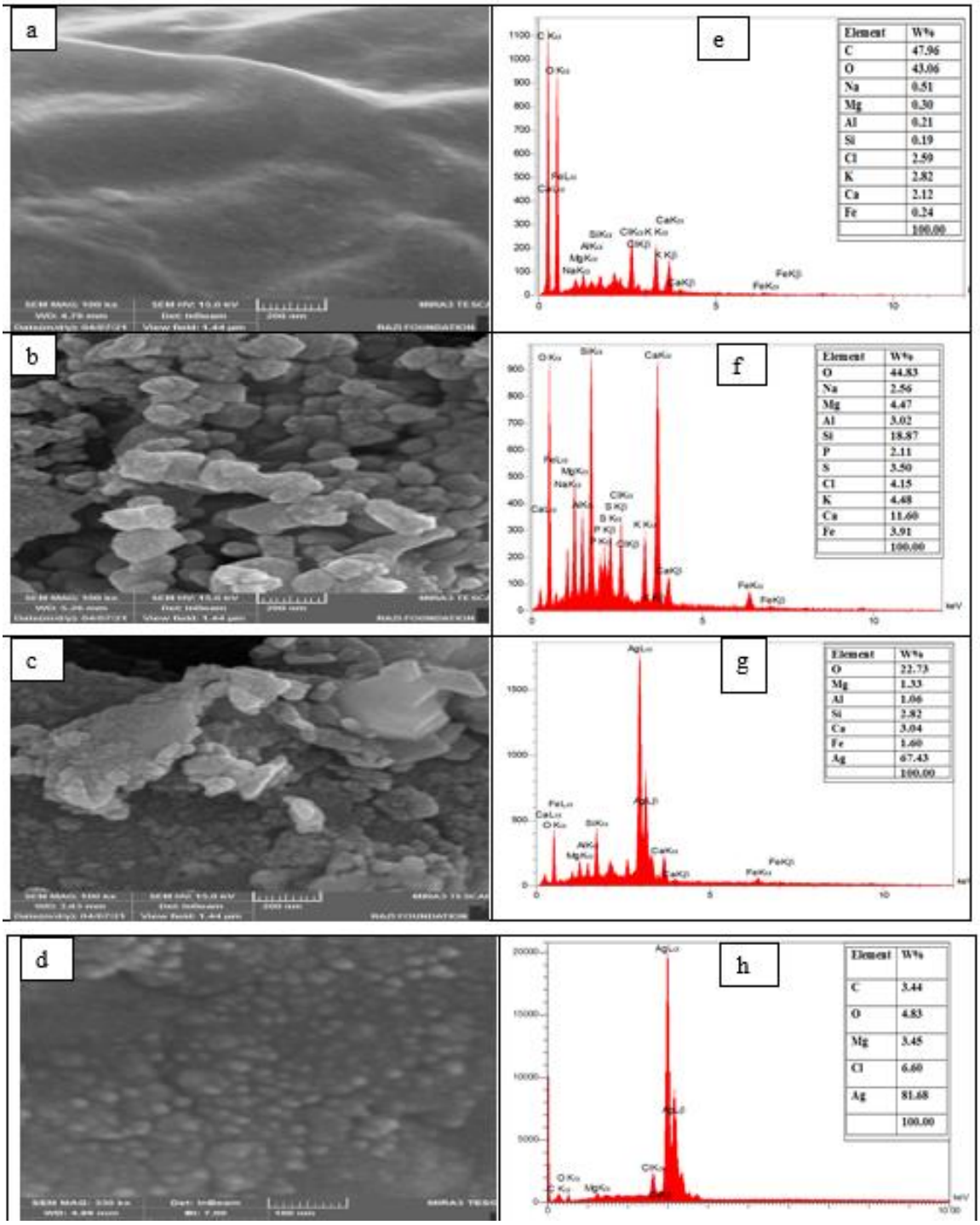

Figure. 1: The FESEM images and EDX .a- before calcination raw EC, b- After calcination raw EC c-Ag Nano Composite, d- Ag Nanoparticle, e- EDX of before calcination raw EC , f- EDX of After calcination raw EC,g- EDX of Ag Nano composite , h- EDX of Ag Nanoparticle

3.1.2-FT-IR spectroscopic analysis

FT-IR spectroscopy has been utilized to identify the functional groups in the (Figure.2-a) before calcination raw EC and after calcination raw EC. In the FT-IR analysis of the before calcination raw EC, bands at 3415, 2927, 1631, 1332, 1045, and 897 cm^{-1} for O–H stretching, C–H asymmetrical stretching, C–H bending, C–O asymmetrical stretching, C–O symmetrical stretching, and C–C stretching vibration [21]. In the FT-IR analysis of the after-calcination raw EC, there is no obvious change in the active groups, as shown in Figure 2-b. These same results have been reported previously [22, 23].

3.1.3-X-Ray Diffraction (XRD):

The XRD diagrams for the prepared sample Ag Nano Composite, AgNP, and EC are shown in Figure (3) (a, b, and C). Figure 1 depicts the X-ray diffraction patterns of the samples (Figure 3c). The typical peaks for EC, When the EC was loaded with silver nitrate and heated, the strong and narrow peak indicates that the product's particles are well crystalline (Figure 3a, b). Silver-like peaks were visible in the XRD patterns. The coordinates for these peaks are 38.01º, 45.65º, 65.28º, and 78.14º. This study builds on previous research [24, 25].

3.1.4-Brunauer-Emmett-Teller (BET) Analysis

The Ag Nano Composite's N_2 adsorption-desorption isotherm is shown in Fig. 4a. It exhibited the appearance of a Type II isotherm, with contributions from both micro and mesopores. In the Ag Nano Composite, the presence of a hysteresis loop at high relative pressure suggested the presence of mesopores, whereas nitrogen uptake at low pressure indicated the presence of micropores. Using the Dubinin-Astakhov method, the micropore surface area was calculated to be 2.1290 cm^3g^{-1} and the limiting micropore volume to be 0.00926 cm^3g^{-1}. The Horvath-Kawazoe had a maximum pore volume of 0.00965 cm^3/g^{-1} cm^3g^{-1} and a median pore width of 0.6173 nm at p/po = 0.175.The Barret-Joyner-Halenda (BJH) pore size model was utilized to obtain Fig. 5c in the adsorption branch of the isotherm. The BJH has an average pore width (V/A) of 15.77 nm. The textural parameters obtained from the analysis of the N_2 physisorption isotherm using various methods, such as Brunauer-Emmett-Teller (BET) surface area and pore size analysis, and the t-plot method, are summarized in Table 1. Mesopores were 0.3953 m^2/g of surface area and had a diameter of 11.952 nm.

3.2. Effect of contact time.

The effect of contact time on the adsorption of thiophene, BT, and DBT on the Ag Nano composite is depicted in Figure 6. At 100 minutes, the amount of thiophene, BT, and DBT regrows as the contact time increases. The equilibrium time for BT and DBT was found to be 150 minutes, while the adsorption of thiophene took approximately 180 minutes to reach equilibrium. During the first 150 minutes, more than 70% of the equilibrium for the eliminated amount of thiophene, BT, and DBT was achieved. Organo sulfur compounds were removed in the following order: T > DBT > BT, with thiophene having the highest percentage removal.

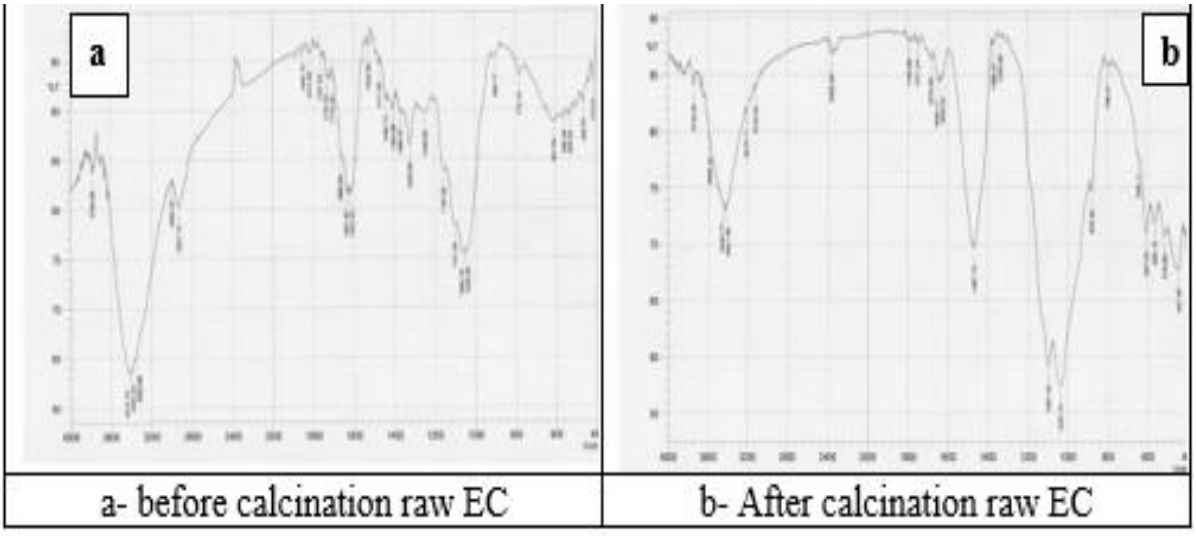

Figure.2-FTIR spectra of the Raw EC. a- before calcination raw EC and b- After calcination raw EC.

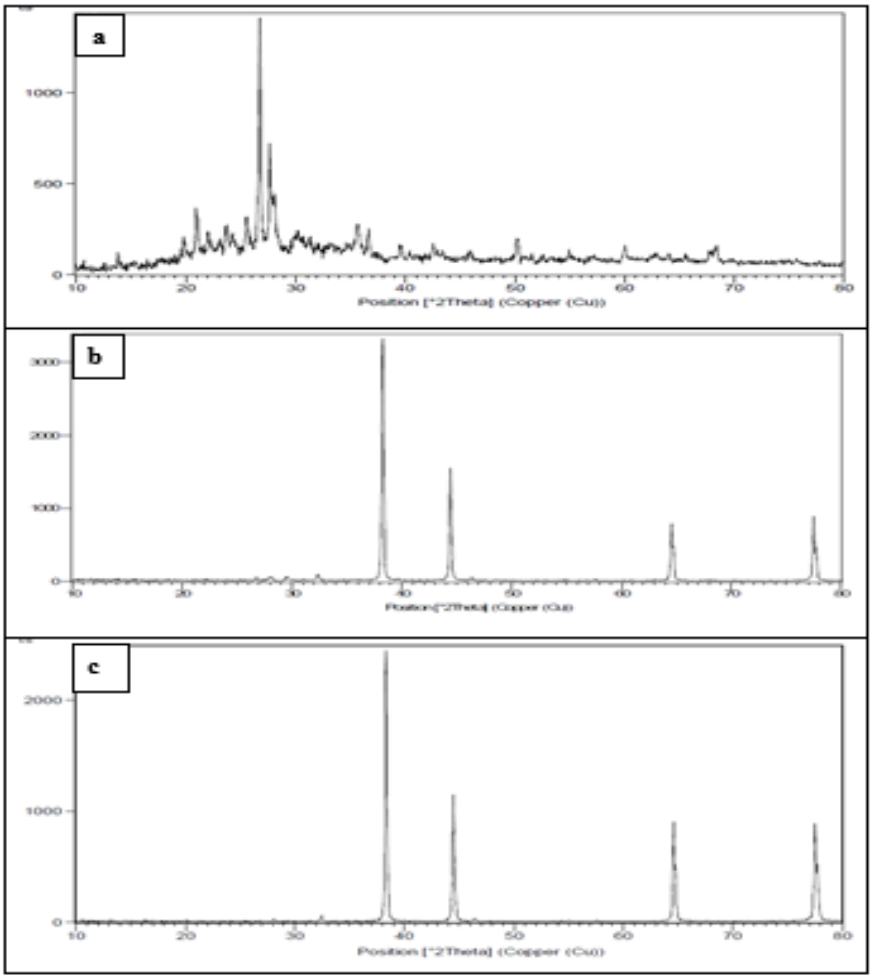

Figure (3): XRD Spectra for (a) EC (b) Ag Nano Composite (c) Ag Nano particle

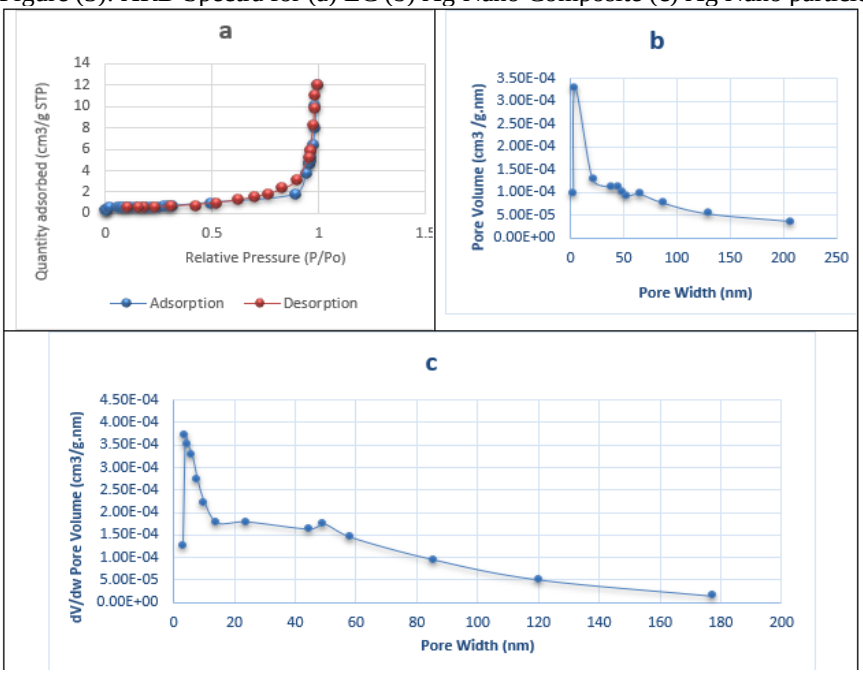

Fig. 4. N_2 adsorption-desorption isotherm (a) pore size distribution (b) and BJH Adsorption dA/dD Pore Area (c) of the Ag Nano Composite

Table 1. Properties of Ag Nano Composite from nitrogen physisorption.

	Surface area m^2/g	Pore volume	Pore diameter	Isotherm type	Hysteresis (p/p^o)	Type of pore
Ag Nano Composite	129.37	0.0072	11.952	II	H3	Meso-porous

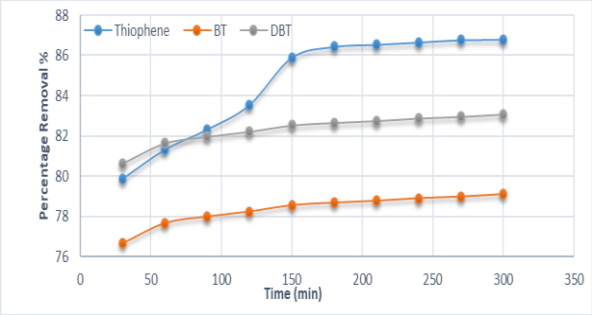

Fig. 5. The effect of contact time on adsorption of Thiophene , BT and DBT

3.3-Effect of Adsorbent Dosage

The effect of the Ag Nano Composite dosage on the percent adsorption of organo-sulfur compounds is shown in Figure 6. When the nanocomposite dose was increased from 0.05 to 0.3 g, the percent adsorption of DBT was around 88% when the initial concentration of thiophene, BT, and DBT was fixed at 80 ppm. Thiophene removal was over 85% in all doses examined, whereas BT removal was around 75%. The order of adsorption of organo sulfur compounds by Ag Nano Composite was thiophene > DBT > BT. There may be more surface area and adsorption sites for the adsorption of Thiophene, BT, and DBT from model oil with more adsorbent dose, but this isn't always the case. [21, 26]

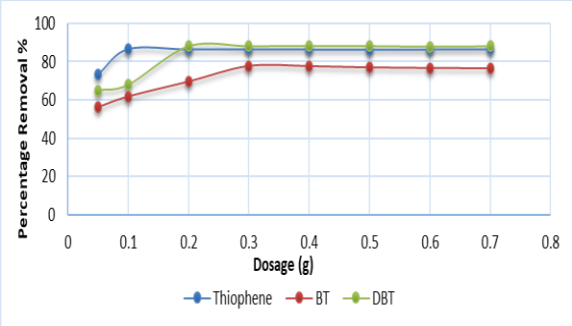

Fig. 6. Effect of adsorbent dosage on adsorption of Thiophene ,BT and DBT.

3.4- Effect of initial concentration.

The effect of Thiophene, BT and DBT concentration on the adsorption of Thiophene, BT and DBT from model oil by Ag Nano Composite was studied by different initial Thiophene, BT and DBT concentration ranges of 80–300 mg/L and the experiment was conducted in a batch process with fixed parameters of adsorbent dosage of 0.2g and time of 150 min. The adsorption of thiophene, BT and DBT from model oil was found to increase with increasing thiophene, BT and DBT concentration.

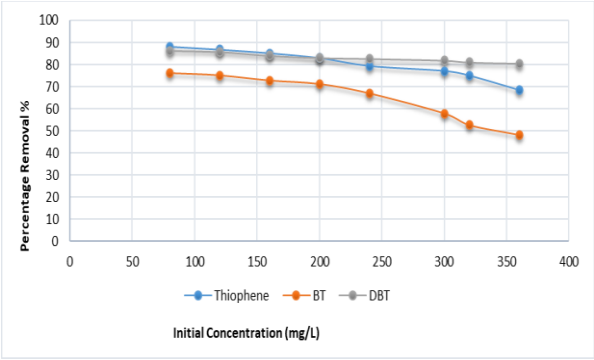

Fig. 7. Effect of initial concentration on adsorption of Thiophene, BT and DBT

2.5. Adsorption isotherms

Langmuir, Freundlich, Temkin, and Dubinin–Radushkevich isotherms were used to describe the equilibrium of the adsorptive desulfurization process. Not only is it helpful when designing and operating the actual adsorption systems, but it also contributes to our understanding of the process of adsorptive desulfurization of diesel fuel, which is commonly thought of as a single-component adsorption.

The Langmuir isotherm model [27] is valid for monolayer adsorption onto a surface containing a finite number of identical sorption sites. It is based on the assumption that every adsorption site is equivalent and independent of whether or not adjacent sites are occupied. The equilibrium expression of the Langmuir model is given by Eq. (3):

$$\frac{1}{q_e} = \left(\frac{1}{K_L Q_m}\right)\frac{1}{C_e} + \frac{1}{Q_m} \quad \ldots\ldots\ldots (3)$$

Where Ce (mg kg−1) indicates the equilibrium concentration of sulfur in model oil, K_L (kgmg−1) represents the Langmuir constant that relates to the affinity of binding sites, and Qm(mg g−1) is the theoretical capacity of the monolayer. The values of K_L and Qmax are calculated from the intercept and slope of the linear plot of ($1/q_e$) versus (1/Ce). The values of Q_{max} and K_L constants and the correlation coefficients for the Langmuir isotherm are presented

in Table 2. The favorability of an adsorption process can be represented in terms of the dimensionless separation factor by the equation (4):

$$R_L = \frac{1}{1+ k_L C_e} \text{..... (4)}$$

This shows that for favorable adsorption, $0 < R_L < 1$, while $R_L > 1$ represents unfavorable adsorption, $R_L = 1$ represents linear adsorption and $R_L = 0$ means the adsorption is irreversible. As estimated value of R_L ranged between 0.066 and 0.357 which means that the adsorption process is favorable.

The Freundlich isotherm [28] is represented by an empirical model that assumes heterogeneous adsorption due to the diversity of adsorption sites and has the following form, Eq. (5):

$$\log q_e = \log K_F + \frac{1}{n} \log C_e \text{ ..... (5)}$$

Where, (L/g) and n are Freundlich constants, which represent the adsorption capacity and intensity, respectively. Based on experimental data, the Freundlich constants are calculated from the intercept and slope of a linear plot of log qe vs log C e. The Langmuir isotherm correlated better than the Freundlich isotherm model for the thiophene, BT, and DBT by the Ag Nano Composite adsorbents. Furthermore, the adsorption capacity of the Ag Nano Composite adsorbent for the removal of thiophene, BT, and DBT was reduced as the temperature increased, indicating that the adsorption process is exothermic. [28]. In accordance with Langmuir and Freundlich isotherms, the results are summarized in Tab. 2 and shown graphically in Figs. 8, 9, and 10. Adsorption equilibrium studies are depicted in Figures 8,9, and 10. Both the Langmuir and Freundlich models match the adsorption isotherms well, with the higher R2 values indicating that the Freundlich isotherm is slightly more suited to coefficient, n, which was less than one in the range of concentrations examined. Physical adsorption is represented by this number. It is well accepted that adsorption on Ag nanocomposite adsorbents is primarily physical in nature, with no chemical relationship found. Another method to describe physical adsorption that's easy to understand and precise is according to Freundlich isotherm isotropy.

The Temkin isotherm [29] have been given by the following linear formulas Eq. (6):

$$q_e = BT \ln AT + BT \ln Ce \text{ .....(6)}$$

Where AT is the equilibrium binding constant (L.g-1) and BT is the Temkin isotherm constant related to adsorption heat (J/mol).The values of AT and BT (in Table 2) can be estimated from the intercept and the slope when plotting qe versus lnCe. The obtained result indicates that the equilibrium data does not fit well with the Temkin isotherm model.

Another equation is used in the Dubinin–Radushkevich (D–R) model [30].the study of isotherms. This model is used to estimate the porosity's apparent free energy and adsorption properties, despite the fact that it does not assume a homogenous surface or a constant sorption potential. It's most typically used in the following ways: Eq. (7):

$$\ln qe = \ln Q_m - K_{D\text{-}R}\varepsilon^2 \text{.....(7)}$$

Where $K_{D\text{-}R}$ is a constant related to the mean free energy of adsorption per mole of ions and Q_m the maximum adsorption capacity. ε is the Polanyi potential can be calculated from equation Eq. (8):

$$\varepsilon = R\ T \ln [1+1/Ce] \text{ ..... (8)}$$

Where R is the gas constant 8.314 $Jmol^{-1}\ K^{-1}$ and *T* is the absolute temperature (K). The slope of the plot of ln q_e versus ε^2 gives K_{D-R} ($mol^2\ kJ^{-2}$) and the intercept yields the adsorption capacity, Q_m ($mg\ g^{-1}$). The adsorption mean free energy (E), can be estimated from the following equation Eq. (9):

$$E = -1/(2B)^{0.5} \text{ .....(9)}$$

When the value of E is less than 6 kJ/mol, the adsorption process can be classified as a type of physical adsorption. If the value of E is in the range of 8 kJ/mol to 16 kJ/mol, the adsorption process is considered a chemisorption process. The Q_m value was found to increase with an increase in temperature.

The value of the regression correlation coefficient suggests that, when compared to the other models studied, the Dubinin-Radushkevich isotherm model does not fit well with the equilibrium experimental data. The mean adsorption energy (E) values were discovered to be within the range of physical adsorption indicated in Tables 2 and 3. In most adsorption methods, the E values range from 0.5 to 5 $kJ\ mol^{-1}$. This means that the adsorption is physical.

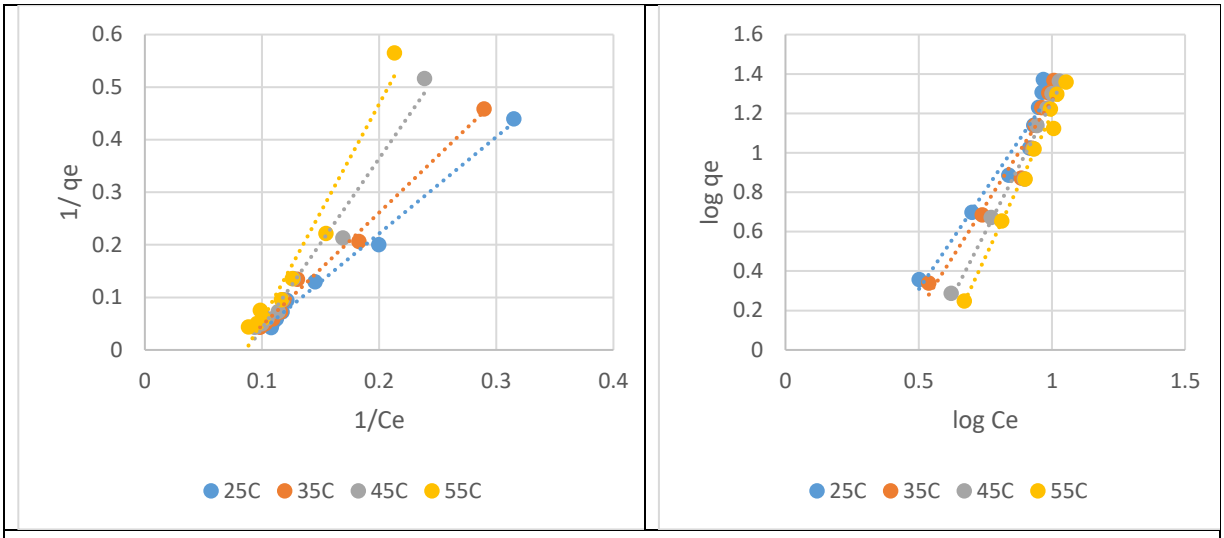

Figure. 8: Langmuir and Freundlich adsorption isotherm for Thiophene at different temperature.

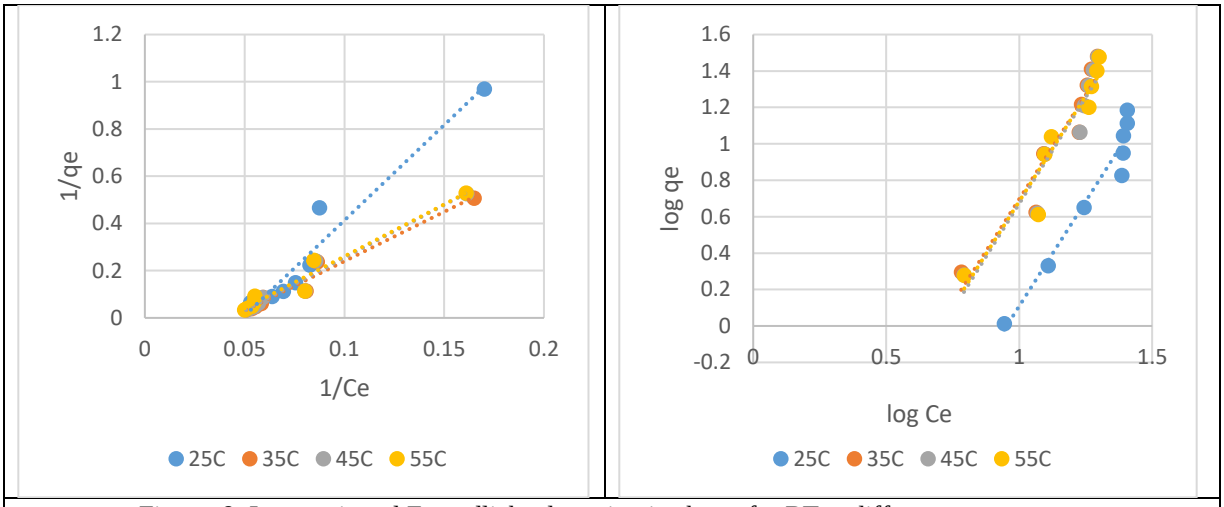

Figure. 9: Langmuir and Freundlich adsorption isotherm for BT at different temperature.

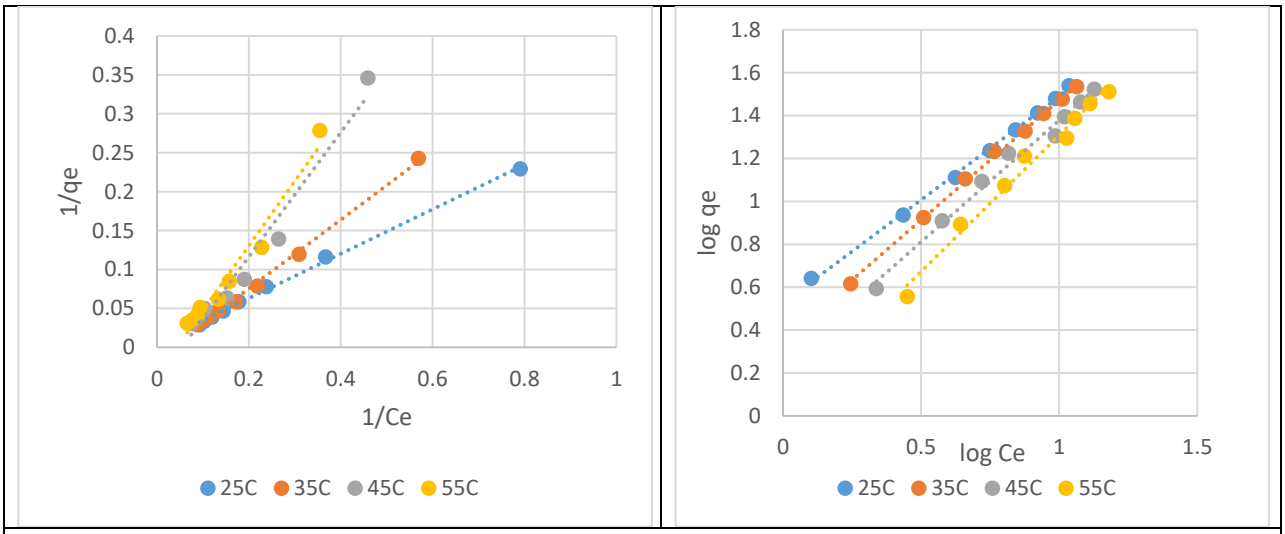

Figure. 10: Langmuir and Freundlich adsorption isotherm for DBT at different temperature.

Table 2- Isotherm model parameters for Thiophene, BT and DBT adsorption at different temperature

Isotherm parameters		Temperature											
		T				**BT**				**DBT**			
Langmuir		**25**	**35**	**45**	**55**	**25**	**35**	**45**	**55**	**25**	**35**	**45**	**55**
Q_m		5.5383	5.303	5.298	5.169	5.805	5.792	5.562	5.162	6.845	5.948	3.559	2.808
K L		0.3111	1.335	1.161	1.268	0.3111	1.33975	1.1601	1.2648	0.3111	1.33975	1.1601	1.2648
R_L		0.2413	0.066	0.077	0.074	0.2413	0.0696	0.0797	0.0734	0.3578	0.2564	0.1654	0.2698
R^2		0.9796	0.9787	0.986	0.969	0.9467	0.9704	0.9721	0.965	0.9673	0.9969	0.9979	0.9674
Freundlich													
K_F		0.15499	0.06148	0.141356	0.232259	0.15499	0.06148	0.2211011	0.212454	1.692319381	1.42504017	1.2759615	1.037797
n		0.497389	0.46856	0.378487	0.344459	0.434555881	0.437426181	0.4282472	0.43204	1.0400416	0.895014771	0.8820676	0.786844
R^2		0.941	0.9447	0.9771	0.9856	0.9486	0.913	0.9182	0.9263	0.9984	0.9985	0.9876	0.9839
Tempkin													
A_T		6.8547	7.0184	7.1807	7.0906	6.854713321	7.0184706	7.180717	7.090622661	6.854713321	7.0184706	7.180717	7.0906226
B_T		12.203	21.242	21.433	20.084	12.203	21.242	21.433	20.084	12.203	21.242	21.433	20.084
b_T		199.63	118.59	121.1	133.7	199.627	118.59251	121.4147	133.7092	199.623207	118.59251	121.4147	133.70952
R^2		0.7621	0.6857	0.681	0.655	0.7621	0.6857	0.6891	0.6505	0.7621	0.6857	0.6891	0.6505
D-R													
Q_m		12.9553	23.114	23.41	22.403	12.956	23.115	23.441	22.405	12.9552356	23.115422	23.44131	22.405355
K_{D-R} x 10^{-6}		2	5	2	2	2	5	2	2	2	5	2	2
E KJmol^{-1}		0.5	0.1	0.5	0.5	0.5	0.1	0.5	0.5	5	1	5	5
R^2		0.7408	0.7468	0.7574	0.7452	0.7408	0.7468	0.7574	0.7452	0.7408	0.7468	0.7574	0.7452

3.6-Kinetics studies

To understand the mechanism of the adsorption process of organosulfur compounds onto Ag Nano Composite in terms of the rate constant order, the experimental adsorption data were analyzed using both pseudo-first order and pseudo-second order kinetic models.The pseudo-first order equation [31] can be written as Eq. (9):

$$\log(q_e - q_t) = \log q_e - \frac{k_1}{2.303} t \quad \text{…….. (9)}$$

qe (mg/g) and qt (mg/g) are the analytes absorbed per unit weight of the adsorbent at equilibrium and at contact time t (min), respectively, while k1 (min-1) is the Lagergren rate constant [31].Figures 11, 12, and 13 illustrate the values of k1 and qe derived from the slopes and intercepts of log (qe−qt) vs t plots in the pseudo-first order model. Tables 3 show that the first-order kinetic model for the adsorption of (Thiophene, DBT, and BT) onto Ag Nano Composite is not correct because of the poor correlation coefficient values and the large difference between the experimental and calculated values of qe. This means that the model is not correct. Pseudo-second order model [32] Adsorption capacity can be represented in a form based on equilibrium. Eq. (10):

$$t/q_t = \frac{1}{k_2 q_e^2} + \frac{1}{q_e}(t) \quad \text{…….. (10)}$$

where k_2 (g mg^{-1} min^{-1}) is the pseudo-second order adsorption rate constant.The amount adsorbed at equilibrium (qe) and second-order rate constant (k_2) were calculated using the slope and intercept of the linear plot of t/qt against t, and the results, together with the correlation coefficients, are given in Tables 3 and Figures 11, 12 and 13. The estimated qe values correspond very well with experimental qe, showing that (Thiophene, BT, and DBT) adsorption onto the Ag Nano Composite adsorbent fits the pseudo-second order kinetic model. A similar phenomenon was observed for the adsorption of DBT onto activated carbon developed from date seeds activated with zinc chloride [33], Mongolian anthracite-based porous activated carbons [34], and coconut shell as an adsorbent [35].

The Elovich equation [36]: was originally utilized to evaluate the chemical adsorption of gas molecules onto heterogeneous solid systems. The Elovich equation can be written as [36]: Eq. (11):

$qt = 1/\beta.\ln(\beta.\alpha) + 1/\beta.\ln(t)$ ……..(11)

Where; qt: is the amount of adsorbed at time t

(min), α (mg/g.min) and β (g/mg) are constants. From the graphs of qt vs ln t, the Elovich coefficients could be calculated. The intercept and slope of the plots of qt against lnt were used to calculate the initial adsorption rate α (mg/g min) and the desorption constant β (g/mg). As shown in Tables 3 and Figures 11, 12 and 13, the correlation coefficients obtained by the Elovich model (R2>0.92) were higher than those obtained by the pseudo first-order model and comparable to those obtained by the pseudo second-order model, indicating that the Elovich model was not applicable to the adsorption of (Thiophene, BT, and DBT) onto Ag Nano Composite.

The intra-particle diffusion model [37] can be expressed by the following Eq. (12):

$qt=kdif\ (t)^{0.5}+BL$……(12)

kdif is the intra-particle diffusion rate constant, and BL is the thickness of the boundary layers. Values of intercept, B_L, give an idea of the thickness of the boundary layer, i. e., the larger the intercept, the greater the boundary layer effect. According to this model, the plot of qt *vs.* $t^{1/2}$ *is shown in* Figures 11, 12, and 13. The correlation coefficients, Table 3, obtained were lower compared to those obtained from the pseudo-second-order kinetic model range between 0.8252-0.971, which indicates low linearity for the adsorption of (Thiophene, BT, and DBT) onto Ag Nano Composite. Higher values of K_{dif} illustrate an enhancement in the rate of adsorption, whereas larger K_{dif} values illustrate a better adsorption mechanism. The most limiting are the diffusion mechanisms, including external diffusion, boundary layer diffusion, and intraparticle diffusion [38]. As a result, the rate-limiting stage of the adsorption process was determined using the intraparticle diffusion model. Intraparticle diffusion is the suitable rate-limiting step if the regression of qt vs $t^{1/2}$ is linear and passes through the origin [39, 40]. Figures 11, 12, and 13 show this quite clearly. Regression was not linear and did not go back to the beginning for the Ag Nano Composite that was being looked into.

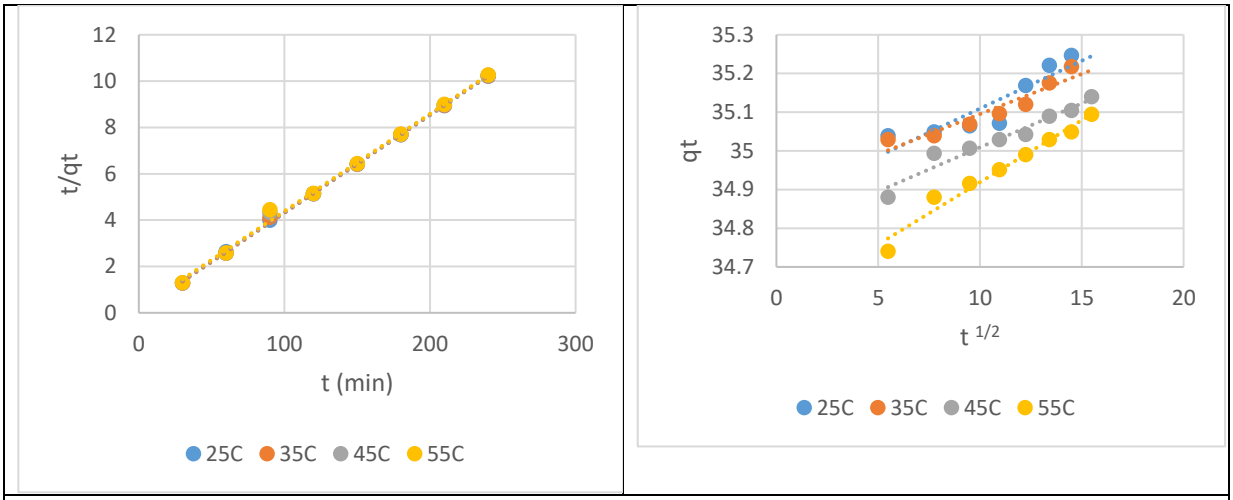

Figure. 11. pseudo-second order and intraparticle diffusion models Adsorption of Thiophene at different temperature

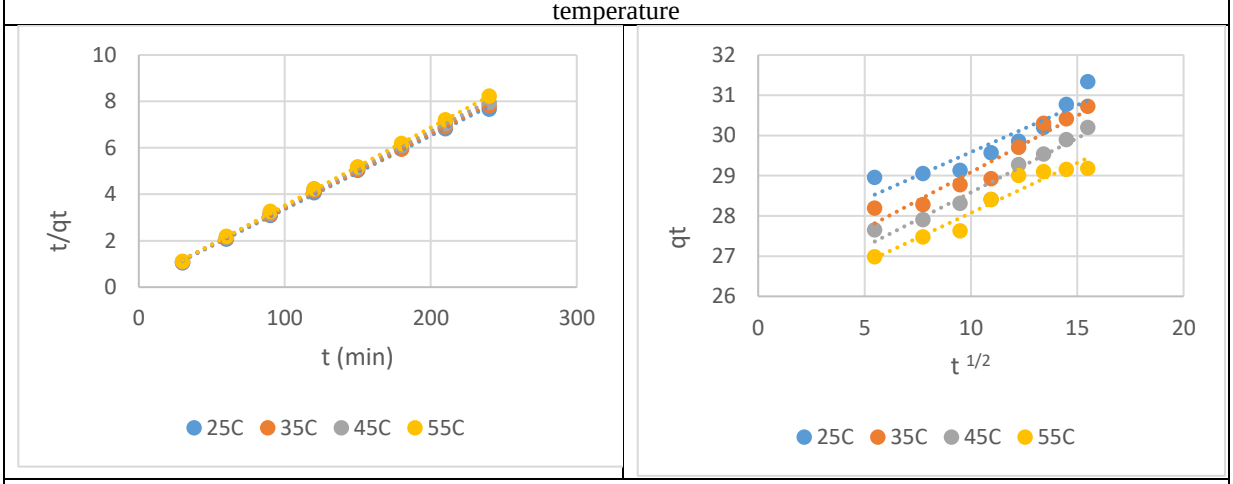

Figure. 12. pseudo-second order and intraparticle diffusion models Adsorption of BT at different temperature

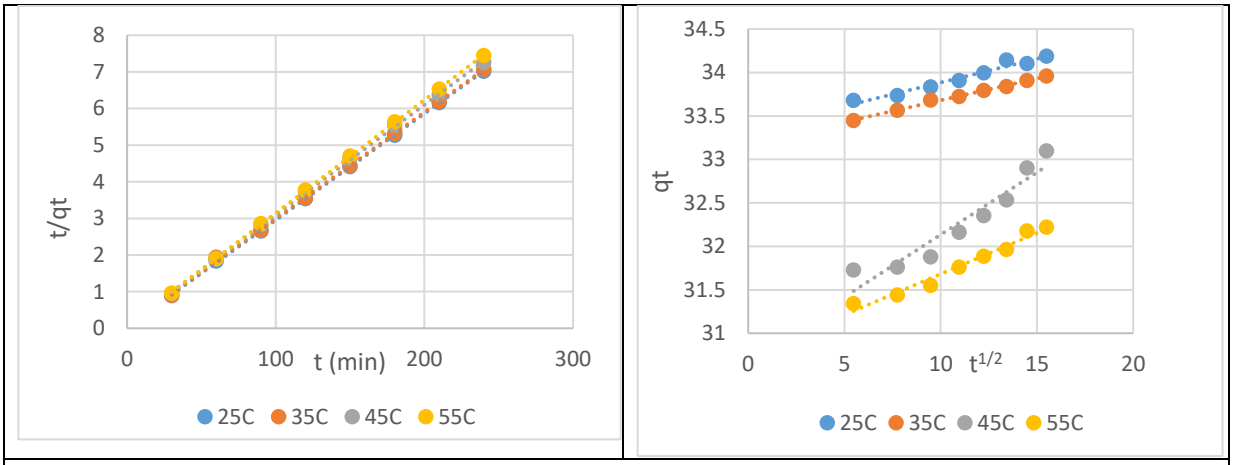

Figure. 13. pseudo-second order and intraparticle diffusion models Adsorption of DBT at different temperature

Table 3 shows the kinetic parameters for the adsorption of Thiophene, BT, and DBT on Ag Nano Composite.

kinetic model	Temperature											
	T				**BT**				**DBT**			
First-order	**25**	**35**	**45**	**55**	**25**	**35**	**45**	**55**	**25**	**35**	**45**	**55**
qe exp.	23.49	23.47	23.42	23.39	31.33	30.71	30.194	29.176	34.188	33.957	33.095	32.22
k1	0.0103	0.0013	0.00161	0.0023	0.0073696	0.0234906	0.0013818	0.0117453	0.0117453	0.0140483	0.0096726	0.0126665
qe	0.28274	0.76955	0.78277	0.64073	0.247413	0.017909	0.054229	0.15920	1.057495	0.534171	0.406606	1.627 08
R^2	0.7112	0.9715	0.8772	0.9065	0.8351	0.8363	0.9623	0.9059	0.9418	0.7974	0.8101	0.8173
Second-order												
k2	0.0194	0.0144	0.011975	0.009343	0.005163	0.004 86	0.005 11	0.007 05	0.017173	0.016321	0.0100	0.0092
qe calc	23.696	23.6966	23.7526	23.8092	31.645569	31.34796	30.67483	29.7616	34.364	32.362	34.013	33.333
R^2	0.9998	0.9991	0.9973	0.9957	0.9987	0.9992	0.9994	0.9997	0.9999	0.9999	0.9994	0.9997
Elovich												
β	8.563	9.487	6.936	8.094	0.938	0.788	0.76	0.821	3.861003	4.12371	2.2441	1.51331
α	0.1309	0.1098	0.1187	0.1202	0.014	0.011	0.09	0.013	0.234	0.265	0.1890	0.1109
R^2	0.8462	0.8987	0.7896	0.987	0.7542	0.8749	0.8545	0.9208	0.9119	0.9793	0.9081	0.8071
intraparticle diffusion												
Kdiff.	0.0207	0.0247	0.0163	0.0321	0.8135	0.2699	0.2811	0.2336	0.0544	0.0499	0.1433	0.0942
BL	34.88	34.862	34.886	34.598	20.635	25.884	26.274	27.249	33.341	33.181	30.701	30.74
R^2	0.9022	0.8252	0.9255	0.9704	0.867	0.9486	0.934	0.957	0.9618	0.9949	0.9091	0.971

3.7-Thermodynamic studies

The adsorption mechanism of thiophene, BT, and DBT onto Ag Nano Composite is evaluated utilizing thermodynamic parameters such as ΔG^o, ΔH^o, and change in ΔS^o (13).

$\Delta Go = RTIn\ K_o$…….. (13)

where ΔGo is the free energy change (kJ mol−1), R is the gas constant (8.314 Jmol−1 K−1), Ko the thermodynamic equilibrium constant and T is the temperature in (K), Where K_0 is the equilibrium constant, C_{solid} mg/L, is the concentration of the adsorbate in the solid phase (adsorbent) at equilibrium, C_{liquid} mg/L, is the equilibrium concentration of the adsorbate in solution, and The values of ΔH^o and ΔS^o can be estimated using Van't Hoff' equation (14);

InK=ΔS/R-ΔH/RT ……(14)

The slope and intercept of the linear plot of lnK vs. 1/T, respectively, yielded ΔH^o and ΔS^o (Fig.14). The values of ΔG^o, ΔH^o, and ΔS^o are shown in Table 4. The fact that ΔG^o is negative suggests that the adsorption occurred spontaneously. The positive value of ΔS^o indicates that the Thiophene, BT, and DBT molecules were adsorbed randomly on the surface of the adsorbent, but the negative value of ΔH^o indicates that the adsorption process was exothermic.

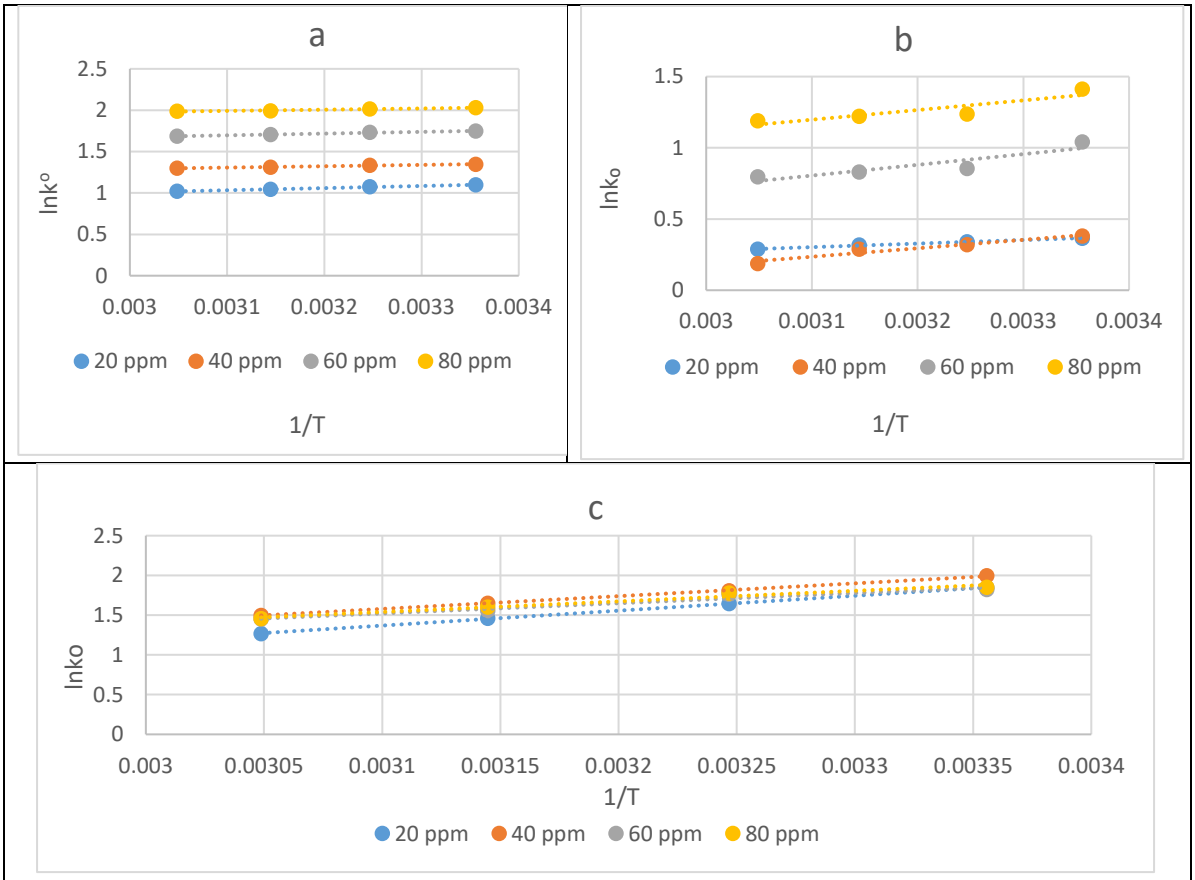

Figure. 14. Van't Hoff plot for the adsorption of Thiophene (a), BT (b) and (c) DBT on the Ag Nano Composite.

Table 4- Thermodynamic parameters for the adsorption of Thiophene, BT and DBT onto Ag Nano Composite.

Conc. mg/L	T				BT				DBT			
	ΔH° KJmol-1	ΔS° KJmol-1	ΔG° KJmol-1	R^2	ΔH° KJmol-1	ΔS° KJmol-1	ΔG° KJmol-1	R^2	ΔH° KJmol-1	ΔS° KJmol-1	ΔG° KJmol-1	R^2
20	-6.144	11.361	-2.715	0.9547	-2.084	9.3898	0.7119	0.9994	-15.800	-37.023	-4.5738	0.9996
40	-1.357	6.6561	-3.337	0.982	-4.931	13.333	-0.942	0.9436	-13.534	-28.342	-4.9401	0.9995
60	-1.734	8.7371	-4.329	0.9883	-6.256	12.702	-2.576	0.8207	-10.751	-20.285	-4.5127	0.9538
80	-1.219	12.781	-5.031	0.9582	-5.629	7.4975	-3.499	0.7926	-11.132	-21.534	-4.5905	0.9704

3.8-Conclusion

This project examined the adsorption of organosulfur compounds utilizing adsorbents made from agricultural waste (Eichhornia crassipes) The Ag Nano Composite was selective for removal of (Thiophene, BT, and DBT in n-heptane). In batch experiments, many parameters such as dose were used (from 0.05-0.4g). (Thiophene, BT, and DBT in n-heptane) starting concentrations (from 10-80 ppm), temperature (from 25-55 C°), While the isotherm demonstrated that Langmuir fit the data more closely for the adsorbents, the Langmuir isotherm correlated better than the Freundlich isotherm model. The kinetic studies revealed that the reaction proceeded via pseudo-second order kinetics. The fact that ΔG^o is negative suggests that the adsorption occurred spontaneously. The positive value of ΔS^o indicates that the thiophene, BT, and DBT molecules were adsorbed randomly on the surface of the adsorbent, but the negative value of ΔH^o indicates that the adsorption process was exothermic.

REFERENCES

[1] Alhamed, Y.A. Bamufleh, H.S., Sulfur removal from model diesel fuel using granular activated carbon from dates' stones activated by $ZnCl_2$, Fuel. 2009, 88, 87–94.

[2] Hanif, M.A., Ibrahim, N., Abdul Jalil, A., Sulfur dioxide removal: An overview of regenerative flue gas desulfurization and factors affecting desulfurization capacity and sorbent regeneration. Environ. Sci. Pollut. Res. 2020. 27 (22), 27515–27540. https://doi.org/10.1007/s11356-020-09191-4.

[3]- Jiang, M. and Ng, F.T.T., Adsorption of benzothiophene on Y zeolites investigated by infrared spectroscopy and flow calorimetry. Catal Today, 2006, 116: 530–536.

[4]- Rekos, K., Kampouraki, Z.C., Panou, C., Baspanelou, A., Triantafyl- lidis, K., Deliyanni, E., Adsorption of DBT and 4,6-DMDBTon nanoporous activated carbons: the role of surface chemistry and the solvent. Environ. Sci. Pollut. Res. 2021. 24,72-84.,https://doi. org/10.1007/s11356-020-08242-0.

[5]- Jeevanandam, P.; Klabunde, K. J.; Tetzle, S. H. Adsorption of Thiophenes out of Hydrocarbons Using Metal Impregnated Nanocrystalline Aluminum Oxide. Microporous Mesoporous Mater. 2005, 79, 101−110.

[6]- Jha, D., Haider, M.B., Kumar, R., Byamba-ochir, N., Shim, W.G., Sivagnanam, B.M., Moon, H., Enhanced Adsorptive Desul-furization Using Mongolian Anthracite- Based Activated Carbon. 2019. ACS Omega 2019, 4, 20844−20853 ,.https://doi.org/10.1021/acsomega.9b03432

[7]- Kumar, S.; Srivastava, V. C.; Badoni, R. P. Oxidative desulfurization by chromium promoted sulfated zirconia. Fuel Process. Technol. 2012, 93, 18−25.

[8]- Irani, Z. A.; Mehrnia, M. R.; Yazdian, F.; Soheily, M. Analysis of petroleum biodesulfurization in an airlift bioreactor using response surface methodology. Bioresour. Technol. 2011, 102, 10585−10591.

[9]- Pasel, J.; Wang, Y.; Hürter, S.; Dahl, R.; Peters, R.; Schedler, U.; Matuschewski, H. Desulfurization of jet fuel by pervaporation. J. Membr. Sci. 2012, 390−391.

[10]- Sadare, Olawumi Oluwafolakemi, Daramola, Michael Olawale, Adsorptive desulfurization of dibenzothiophene (DBT) in model petroleum distillate using functionalized carbon nanotubes. Envi- ron. Sci. Pollut. Res. 2019. 26 (32), 32746–32758. https://doi.org/10.1007/s11356-019-05953-x.

[11]- Danmaliki, G.I., Saleh, T.A., 2017. Effects of bimetallic Ce / Fe nanoparticles on the desulfurization of thiophenes using activated carbon. Chem. Eng. J. 307, 914–927. https://doi.org/10.1016/j.cej.2016.08.143.

[12]- Lin, L.; Zhang, Y.; Zhang, H.; Lu, F. Adsorption and solvent desorption behavior of ion-exchanged modified Y zeolites for sulfur removal and for fuel cell applications. J. Colloid Interface Sci. 2011, 360, 753−759.

[13]. Husseien, M., Amer, A., El-Maghraby, A. & Hamedallah, N. Oil spill removal from water by using corn stalk: factors affecting sorption process. International Journal of Environment and Waste Management .2015, 16, 281–292

[14]. Villamagna, A. & Murphy, B. Ecological and socio-economic impacts of invasive water hyacinth (Eichhornia crassipes): a review. Freshwater biology. 2010, 55, 282–298 .

[15]. Ratan, J. K., Kaur, M. & Adiraju, B. Synthesis of activated carbon from agricultural waste using a simple method: Characterization, parametric and isotherms study. Materials Today: Proceedings .2018,5, 3334–3345 .

[16]- Hassan Shokry,Marwa Elkady,Eslam Salama, "Eco-friendly magnetic activated carbon nano-hybrid for facile oil spills separation" Scientific Reports, (2020) ,10(1),10265 .| https://doi.org/10.1038/s41598-020-67231-y .

[17]-Nada S. Ahmedzeki ,Salah M. Ali , and Sarah R. Al-Karkhi , Synthesis and Characterization of Tri-Composite Activated Carbon, Iraqi Journal of Chemical and Petroleum Engineering.2017,18(3), 49 – 58,

[18]- A.A. Olajirea,*, J.J. Abidemib, A. Lateefc, N.U. BensondAdsorptive desulphurization of model oil by Ag nanoparticles-modified activated carbon prepared from brewer's spent grains, Journal of Environmental Chemical Engineering .2017, 5 147–159.

[19]- Elham S. Moosavi, Seyed A. Dastgheib and Ramin Karimzadeh, Adsorption of Thiophenic Compounds from Model Diesel Fuel,, Energies 2012, 5, 4233-4250; doi:10.3390/en5104233. Using Copper and Nickel Impregnated Activated Carbons.

[20]- Tippayawat, P.; Phromviyo, N.; Boueroy, P.; Chompoosor, A. Green synthesis of silver nanoparticles in aloe vera plant extract prepared by a hydrothermal method and their synergistic antibacterial activity. PeerJ .2016, 4(e2589), 1-15.

[21] Naeem S., Baheti V., Militky J., Removal of textile dye methylene blue from liquid-phase by activated carbon from Aloe Vera wastes, Int J Eng Tech Res.2016, , 9(1), 1-8.

[22] Runjuan Zhou*, Ming Zhang, Jinhong Zhou & Jinpeng Wang, Optimization of biochar preparation from the stem of Eichhornia crassipes using response surface methodology on adsorption of Cd^{2+}, Scientific Reports . 2019 ,9,17538. https://doi.org/10.1038/s41598-019-54105-1 ,www.nature.com/scientificreports.

[23] R. P. Premalatha1, E. Parameswari, P. Malarvizhi1, S. Avudainayagam and V. Davamani, Sequestration of Hexavalent Chromium from Aqueous Medium Using Biochar Prepared from Water Hyacinth Biomass, Chemical Science International Journal. 2018,22(3),1-15.

[24] Zakia Kanwal1, Muhammad Akram Raza, Saira Riaz, Saher Manzoor, Asima Tayyeb, Imran Sajid4 and Shahzad Naseem, Synthesis and characterization of silver nanoparticle-decorated cobalt nanocomposites(Co@AgNPs) and their density-dependent antibacterial activity, R. Soc. open sci,2019, 6: 182135. http://dx.doi.org/10.1098/rsos.182135,2019.

[25] G.M. Srirangam1 and K. Parameswara Rao, Synthesis and characterization of silver nanoparticles from the leaf extract of malachra capitata (L), J Rasayan . Chem. 2017, 10(1), 46-53 .http://dx.doi.org/10.7324/RJC.2017.1011548.

[26] A.A. Adeyi, I.T. Popoola, A.S. Yusuff, A.S. Olateju, Kinetics analysis and dosage effect of manganese dioxide adsorbent on desulphurization of crude oil, J. Bioprocess. Chem. Eng. 2014, 2, 1–6.

[27] Ayawei, N., Ebelegi, A. N., & Wankasi, D. (2017). Modelling and interpretation of adsorption isotherms. Journal of chemistry, 2017,1-11 https://doi.org/10.1155/2017/3039817.

[28] Freundlich H., die U ,adsorption in losungen, Zeitschrift fur Physikalische Chemie-Leipzig .1906, 57 385–470.

[29] Bouatay F., Dridi S. , Mhenni M.F., "Valorization of Tunisian pottery clay onto basic dyes adsorption", International Journal of Environmental Researches, **2014**, 8, 4, 1053-1066.

[30] Collins O.N., Elijah O.C., Okechukwu D.O., "Adsorption of dye (crystal violet) on an acid modified non-conventional adsorbent'', Journal of Chemical Technology and Metallurgy, **2019**, 45, 1, 95-110.

[31] Lagergren S., About the theory of so-called adsorption of soluble substances (in German), Kungliga Svenska Vetenskapsakademiens Handlingar .1898, 24 (4) 1–39.

[32] Weber.J., Morris.j., Kinetics of adsorption carbon from solutions, J. Sanit. Eng. Div. Am. Soc. Civ. Eng. 1963, 89 31–60.

[33]- Musa O. Azeez, Abdulkadir Tanimu, Khalid Alhooshani, Saheed A. Ganiyu , Synergistic effect of nitrogen and molybdenum onactivated carbon matrix for selective adsorptive Desulfurization: Insights into surface chemistry modification, Arabian Journal of Chemistry .2022, 15, 103454.

[34] Divyam J., Mohd B., Rakesh K., Narandalai B., Wang G., Balathanigaimani Marriyappan S., Hee M., Enhanced Adsorptive Desulfurization Using Mongolian Anthracite Based Activated Carbon, ACS Omega 2019, 4, 20844-20853. DOI: 10.1021/acsomega.9b03432

[35] Nurul S., Azil B., Mohd A., Raja R., Ali H ., Khairul A., Khudzir I., Sulfur dioxid gas adsorption study using mixed activated carbon from different biomass, International Journal of Technology. 2018, 6: 1121-1131.

[36] Martins R.J., Vilar V.J., Boaventura R.A., "Kinetic modelling of cadmium and lead removal by aquatic mosses'', Brazilian Journal of Chemical Engineering, 2014, 31, 1, 229-242.

[37]- Itodo A.U., Abdulrahman F.W., Hassan L.G., Maigandi S.A. Itodo H.U., "Intraparticle diffusion and intraparticulate diffusivities of herbicide on derived activated carbon'', Researcher, 2010, 2, 74-86.

[38] Marko Muzic, Katica Sertic-Bionda, Zoran Gomzi**,** Kinetic and Statistical Studies of Adsorptive Desulfurization of Diesel Fuel on Commercial
Activated Carbons, *Chem. Eng. Technol.* **2008**, *31*(3), 355–364.

[39] Ozcan A., Ozcan A. S., *J. Hazard. Mater*. **2005**, *125*, 252. DOI: 10.1016/j.jhazmat.2005.05.039.

[40] Kannan K., Sundaram M. M., Dyes Pigm. **2001**, 51, 25. DOI: PII: S0143-7208 (01)00056-0.
[41]- Rojas G., Silva J., Flores J. A., Rodriguez A., Ly M., Maldonado H Adsorption of chromium onto cross-linked chitosan, Separation and Purification Technology.2005, 44,31-36 .